

Hadron interferences in the proton-induced coherent η -meson-production reaction on a scalar-isovector nucleus

Swapan Das*

Nuclear Physics Division, Bhabha Atomic Research Centre, Mumbai 400085, India

(Received 3 March 2015; revised manuscript received 14 May 2015; published 21 July 2015)

The coherent η -meson energy E_η distribution spectra in proton nucleus reactions have been calculated to investigate the π^0 - η mesons' interference, in addition to the study of resonance N^* dynamics in the nucleus. The elementary reaction occurring in the nucleus is assumed to proceed as $pN \rightarrow pN^*$; $N^* \rightarrow N\eta$. Born terms in the intermediate state are also considered. In a scalar-isovector nucleus, this reaction occurs because of π^0 - and η -meson exchange interactions for the forward going proton and the η meson; other meson exchange potentials do not contribute to this process. The sensitivity of the cross section to the hadron nucleus interactions and the beam energy dependence of the cross section are studied for this reaction.

DOI: [10.1103/PhysRevC.92.014621](https://doi.org/10.1103/PhysRevC.92.014621)

PACS number(s): 25.40.Ve, 13.30.Eg, 13.60.Le

I. INTRODUCTION

One of the current interests in intermediate energy nuclear and particle reactions is to explore the dynamics of η meson that can be produced either in a (quasi)bound state or in continuum [1]. Several data sets for the η -meson production in hadron-induced reactions are available from various laboratories, like COSY [2] (see the references therein), SATURNE [3], Los Alamos [4], and Brookhaven [5]. The production of η mesons in heavy-ion collisions was reported by GSI [6]. Due to the advent of high-duty electron accelerators at Jefferson Laboratory, Bates, MAMI, ELSA, etc., good quality data have been obtained for the photo- and electroproduction of η mesons [7]. These accelerator facilities, along with the newly developed sophisticated detecting systems, provide ample scope to investigate the physics of η mesons.

The study of reaction mechanisms for η -meson production opens various avenues to learn about many exciting aspects of physics. Large and attractive ηN scattering length near the threshold production of this meson predicts the existence of a new hadronic atom, i.e., the (quasi) η -mesic nucleus [8,9]. The π^0 - η mixing has been shown to occur in charge symmetry breaking (CSB) reactions [10]. Being an isoscalar particle, the η meson can excite a nucleon to $I = \frac{1}{2}$ resonances. Specifically, the $N(1535)$ resonance, $I(J^P) = \frac{1}{2}(\frac{1}{2}^+)$, has a large decay branching ratio to η meson and nucleon at the pole mass. Therefore, the η -meson production in the nuclear reaction is considered as a potential tool to investigate the dynamics of $N(1535)$ in the nucleus. Of course, this reaction can also be used to study the η -meson nucleus interaction in the final state [11,12].

The η meson can be produced through the hadronic interaction by scattering off the pion or proton on the proton or nuclear target. Theoretical studies of these reactions, as done by various authors [13–15], show that the η meson in the final state arises because of the decay of $N(1535)$ produced in the intermediate state. Sometime back, Lopez Alvarez and Oset [16] studied coherent η -meson production in the (p, p')

reaction on the spin-isospin saturated nuclei: $p + A(\text{gs}) \rightarrow p' + A(\text{gs}) + \eta$. The elementary reaction in the nucleus is considered to be $pN \rightarrow p'N(1535)$; $N(1535) \rightarrow N\eta$. The resonance $N(1535)$ in the intermediate state is produced due to the η -meson (a pseudoscalar-isoscalar meson) exchange interaction or potential only, specifically, for the forward going proton and η meson. Contributions from other meson exchange potentials, as discussed in Ref. [16], vanish for this reaction.

The importance of the $N(1520)$ resonance in the η -meson-production reaction is discussed in Ref. [17]. The earlier value of the coupling constant $f_{\eta NN(1520)}$ was 6.72, whereas the latest value of it is 9.98. This coupling constant is much larger than the $\eta NN(1535)$ coupling constant: $g_{\eta NN(1535)} \simeq 1.86$. The η -meson-production cross section due to $N(1520)$ in the abovementioned reaction is increased by a factor of ~ 5 because of the enhancement in $f_{\eta NN(1520)}$. As shown in Fig. 2 of Ref. [17], the $N^* \rightarrow N\eta$ decay probability of $N(1520)$ rises sharply over that of $N(1535)$ with the increase in resonance mass. In fact, this probability for $N(1520)$ is larger than that for $N(1535)$ at higher energy. It is also shown in Ref. [17] that the contribution of the $N(1535)$ resonance to the considered reaction is the largest at low energy, i.e., ~ 1 GeV, provided $f_{\eta NN(1520)}$ is taken to be equal to 6.72. In the multi-GeV region, the distinctly dominant contribution to the reaction (quoted above) arises due to the $N(1520)$ resonance. In addition to these, the contributions to the cross section due to the Born terms and other resonances [whose $N\eta$ branching ratio is $\geq 4\%$ [18], i.e., $N(1650)$, $N(1710)$, and $N(1720)$ resonances] are also presented in this work.

It should be mentioned that both π and η mesons are pseudoscalar particles but the π^0 exchange potential cannot contribute to the abovementioned reaction since it is an isovector meson and the quoted reaction involves an isoscalar nucleus. In contrast to this, both π^0 - and η -meson exchange interactions can contribute to the $p \rightarrow N^*$ excitation in the spin-saturated isovector nucleus. Therefore, the coherent η -meson production in the (p, p') reaction in the scalar-isovector nucleus can be used to study the contribution of π^0 - and η -meson exchange potentials (along with their interference) to the reaction. In addition, this reaction can also be used to investigate the dynamics of Born terms and nucleonic resonances, similar to those presented in Ref. [17].

*swapand@barc.gov.in

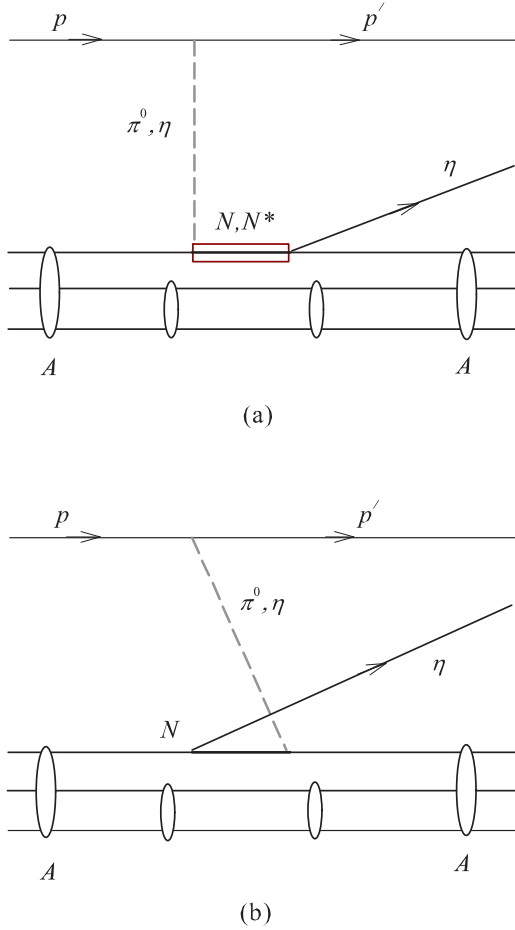


FIG. 1. (Color online) Schematic diagrams describing the mechanism of the considered reaction (see text): (a) direct (or postemission) and (b) cross (or preemission) diagrams.

The diagrammatic presentation of the considered reaction is exhibited in Fig. 1. Figure 1(a) describes the direct or postemission mechanism for the reaction where both the Born term N (represented by the bold solid line inside the rectangle) and the resonance term N^* (shown by the rectangle) have been incorporated. Figure 1(b) elucidates the cross or postemission mechanism for the reaction where only the Born term N is considered, because the contribution of the resonance N^* term in this case can be neglected compared with that described in Fig. 1(a) [19].

In the coherent meson-production reaction, the meson in the final state, i.e., the η meson in the considered reaction, takes away almost the whole energy transferred to the nucleus, i.e., $E_\eta \approx (E_p - E_{p'})$, whereas the momentum of this meson is adjusted by the recoiling nucleus. The state of the nucleus does not change in this reaction. In the formalism for the coherent η -meson production in the proton nucleus (scalar-isovector) reaction, the distorted wave functions of protons and η meson are expressed by the eikonal form. The optical potentials (appearing in the N^* propagator as well as in the distorted wave functions of protons) are worked out using the “ $t_Q(\mathbf{r})$ ” approximation. The η -meson optical potential is evaluated following that given in Ref. [16]. The cross section for the

coherent η -meson energy E_η distribution in the above reaction is calculated to study various aspects of it, which include (i) the resonance dynamics, (ii) the interference of π^0 - and η -meson-exchange interactions, (iii) the sensitivity of the cross section to the hadron nucleus interaction (optical potential), and (iv) the beam energy dependence of the cross section.

II. FORMALISM

The Lagrangian \mathcal{L} representing the meson-baryon interaction depends on their spin and parity. For the pseudoscalar (0^-) meson (i.e., π or η meson) coupling to the resonances in the considered reaction, the forms for \mathcal{L} are presented below [20,21]. For the $\frac{1}{2}^+$ particle [i.e., $N(940)$ or $N^* \equiv N(1710)$], they can be expressed as

$$\begin{aligned}\mathcal{L}_{\pi NN} &= -i g_\pi F_\pi(q^2) \bar{N} \gamma_5 \boldsymbol{\tau} N \cdot \boldsymbol{\pi}, \\ \mathcal{L}_{\eta NN} &= -i g_\eta F_\eta(q^2) \bar{N} \gamma_5 N \eta, \\ \mathcal{L}_{\pi NN^*} &= -i g_\pi^* F_\pi^*(q^2) \bar{N}^* \gamma_5 \boldsymbol{\tau} N \cdot \boldsymbol{\pi}, \\ \mathcal{L}_{\eta NN^*} &= -i g_\eta^* F_\eta^*(q^2) \bar{N}^* \gamma_5 N \eta,\end{aligned}\quad (1)$$

where g_π [$\pi NN(940)$ coupling constant] $\simeq 13.4$ [22], g_η [$\eta NN(940)$ coupling constant] $\simeq 7.93$ [23], g_π^* [$\pi NN(1710)$ coupling constant] = 1.2, and g_η^* ($\eta NN(1710)$ coupling constant) $\simeq 4.26$. For the $\frac{1}{2}^-$ resonance N^* , i.e., $N(1535)$ and $N(1650)$, the forms for \mathcal{L} are given by

$$\begin{aligned}\mathcal{L}_{\pi NN^*} &= -i g_\pi^* F_\pi^*(q^2) \bar{N}^* \boldsymbol{\tau} N \cdot \boldsymbol{\pi}, \\ \mathcal{L}_{\eta NN^*} &= -i g_\eta^* F_\eta^*(q^2) \bar{N}^* N \eta,\end{aligned}\quad (2)$$

where $g_\pi^* \simeq 0.71$ and $g_\eta^* \simeq 1.86$ for $N(1535)$, and $g_\pi^* \simeq 0.83$ and $g_\eta^* \simeq 0.67$ for $N(1650)$. For $N(1520)\frac{3}{2}^-$, the forms for \mathcal{L} can be written as

$$\begin{aligned}\mathcal{L}_{\pi NN^*} &= \frac{f_\pi^*}{m_\eta} F_\pi^*(q^2) \bar{N}^{*\mu} \gamma_5 \boldsymbol{\tau} N \cdot \partial_\mu \boldsymbol{\pi}, \\ \mathcal{L}_{\eta NN^*} &= \frac{f_\eta^*}{m_\eta} F_\eta^*(q^2) \bar{N}^{*\mu} \gamma_5 N \partial_\mu \eta,\end{aligned}\quad (3)$$

where $f_\pi^* = 6.54$ and $f_\eta^* \simeq 9.98$. For the $\frac{3}{2}^+$ resonance [24], i.e., $N^* \equiv N(1720)$, the forms for \mathcal{L} are given by

$$\begin{aligned}\mathcal{L}_{\pi NN^*} &= \frac{f_\pi^*}{m_\eta} F_\pi^*(q^2) \bar{N}^{*\mu} \boldsymbol{\tau} N \cdot \partial_\mu \boldsymbol{\pi}, \\ \mathcal{L}_{\eta NN^*} &= \frac{f_\eta^*}{m_\eta} F_\eta^*(q^2) \bar{N}^{*\mu} N \partial_\mu \eta,\end{aligned}\quad (4)$$

where $f_\pi^* \simeq 0.64$ and $f_\eta^* \simeq 1.15$. The coupling constants (i.e., g^* s and f^* s) are extracted from the measured decay widths of the resonances, i.e., $N^* \rightarrow N\pi$ and $N^* \rightarrow N\eta$ [18]. $F_{\pi(\eta)}(q^2)$ and $F_{\pi(\eta)}^*(q^2)$ are $\pi(\eta)NN$ and $\pi(\eta)NN^*$ form factors at the respective vertices [23]:

$$F_M(q^2) = F_M^*(q^2) = \frac{\Lambda_M^2 - m_M^2}{\Lambda_M^2 - q^2} \quad (M \equiv \pi^0, \eta). \quad (5)$$

In this equation, $q^2 [= q_0^2 - \mathbf{q}^2]$ is the four-momentum transfer to the nucleus, i.e., $q_0 = E_p - E_{p'}$ and $\mathbf{q} = \mathbf{k}_p - \mathbf{k}_{p'}$. The form factors are normalized to unity when the mesons are on

TABLE I. $\Lambda_{N(N^*)}(S)$ for spin $S = \frac{1}{2}$ and $\frac{3}{2}$ fermions.

Spin(S)	$\Lambda(S)$
$\frac{1}{2}$	$\{\mathbf{k} + m_{N^*}\}$
$\frac{3}{2}$	$\{\mathbf{k} + m_{N^*}\} [g_v^\mu - \frac{\gamma^\mu \gamma_\nu}{3} - \frac{\gamma^\mu k_\nu - \gamma^\nu k_\mu}{3m_{N^*}} - \frac{2k^\mu k_\nu}{3m_{N^*}^2}]$

shell. Values of the length parameters are $\Lambda_\pi = 1.3$ GeV and $\Lambda_\eta = 1.5$ GeV [23].

The T matrix T_{fi} of the considered reaction can be written as

$$T_{fi} = \sum_{M=\pi^0, \eta} [T_B(M) + T_{N^*}(M)], \quad (6)$$

where $T_B(M)$ represents the T matrix due to Born terms arising because of either the π^0 -meson exchange potential or the η -meson exchange potential. It is given by

$$T_B(M) = \Gamma_{NN\eta} \Lambda_N(S) V_M(q) \int d\mathbf{r} \chi^{(-)*}(\mathbf{k}_\eta, \mathbf{r}) \times G_{N\varrho_I}(\mathbf{r}) \chi^{(-)*}(\mathbf{k}_{p'}, \mathbf{r}) \chi^{(+)}(\mathbf{k}_p, \mathbf{r}). \quad (7)$$

The factor ϱ_I in the above equation denotes the isospin-averaged density distribution of the nucleus. χ s represent the wave functions for the continuum particles. These quantities are elaborated later. $\Gamma_{NN\eta}$ describes the interaction for the emission of η mesons at the ηNN vertex in the final state. $V_M(q)$ represents the pseudoscalar meson (i.e., $M \equiv \pi^0$ or η) exchange potential between the beam proton and a nucleon in the nucleus, shown by the dashed line in Fig. 1: $V_M(q) = \Gamma_{MNN} G_M(q^2) \Gamma_{Mpp'}$. In this equation, Γ_{MNN} denotes the interaction at MNN vertex (in the nucleus), whereas $\Gamma_{Mpp'}$ represents that at the Mpp' vertex (i.e., meson-projectile-ejectile vertex). These Γ s are addressed by $\mathcal{L}_{\pi(\eta)NN}$ in Eq. (1). $G_M(q^2)$ is the virtual $\pi^0(\eta)$ -meson propagator, i.e., $G_{\pi^0(\eta)}(q^2) = -\frac{1}{m_{\pi^0(\eta)}^2 - q^2}$. $\Lambda_N(S)$ represents the spin (S)-dependent part of the nucleon propagator, i.e., $\Lambda_N(S = \frac{1}{2})$ in Table I. The scalar part of the nucleon Born propagator G_N for direct (D) and cross (C) channels, as illustrated in Fig. 1, are given by

$$G_N^D = \frac{1}{s - m_N^2}, \quad G_N^C = \frac{1}{u - m_N^2}, \quad (8)$$

where s and u are invariant Mandelstam kinematical variables (see page 28 in Ref. [22]).

The resonance contribution to the T matrix, i.e., $T_{N^*}(M)$ in Eq. (6), is given by

$$T_{N^*}(M) = \sum_{N^*} \Gamma_{N^* \rightarrow N\eta} \Lambda_{N^*}(S) V_M(q) \int d\mathbf{r} \chi^{(-)*}(\mathbf{k}_\eta, \mathbf{r}) \times G_{N^* \varrho_I}(\mathbf{r}) \chi^{(-)*}(\mathbf{k}_{p'}, \mathbf{r}) \chi^{(+)}(\mathbf{k}_p, \mathbf{r}). \quad (9)$$

$\varrho_I(\mathbf{r})$ and χ s also appear in Eq. (7). $\Gamma_{N^* \rightarrow N\eta}$ denotes $N^* \rightarrow N\eta$ decay in the final state. $V_M(q)$ in this case is given by $V_M(q) = \Gamma_{MNN^*} G_M(q^2) \Gamma_{Mpp'}$, where Γ_{MNN^*} represents the interaction at the MNN^* vertex (in the nucleus) described by $\mathcal{L}_{\pi(\eta)NN^*}$ in Eqs. (1)–(4). Other quantities in $V_M(q)$ are

TABLE II. Resonance width $\Gamma_{N^*}(m_{N^*})$ at pole mass m_{N^*} in MeV [18].

Resonance N^*	$\Gamma_{N^*}(m_{N^*})$
$N(1520)$	115
$N(1535)$	150
$N(1650)$	150
$N(1710)$	100
$N(1720)$	250

already defined below Eq. (7). The spin-dependent part of the N^* propagator $\Lambda_{N^*}(S)$ is expressed in Table I. The scalar part of this propagator, G_{N^*} in Eq. (9), according to Fig. 1(a), can be expressed as

$$G_{N^*}(m) = \frac{1}{m^2 - m_{N^*}^2 + im_{N^*} \Gamma_{N^*}(m)}, \quad (10)$$

where m_{N^*} is the pole mass of the resonance N^* . $m(\equiv s)$ is the invariant mass of the η meson and the nucleon, arising due to the decay of N^* . Because the cross or premission channel in this case (as mentioned earlier) can be neglected, the T matrix for it is not considered. Indeed, this equation represents the resonance propagator in the free space because the resonance nucleus interaction in it (which is considered later) is omitted.

$\Gamma_{N^*}(m)$ in Eq. (10) represents the total width of N^* for its mass equal to m . The experimentally determined values of it at its pole mass, i.e., $m = m_{N^*}$, for all considered resonances are listed in Table II. Since the resonance N^* can decay into various channels, $\Gamma_{N^*}(m)$ consists of partial decay widths as written below [18].

For the $N^* \equiv N(1520)$ resonance,

$$\Gamma_{N^*}(m) = \Gamma_{N^* \rightarrow N\pi}(m)|_{l=2} + \Gamma_{N^* \rightarrow \Delta\pi}(m)|_{l=0} + \Gamma_{N^* \rightarrow \Delta\pi}(m)|_{l=2} + \Gamma_{N^* \rightarrow N\eta}(m)|_{l=2}, \quad (11)$$

where l is the angular momentum associated with the decay, $\Gamma_{N^* \rightarrow N\pi}(m)|_{l=2} \approx 0.65\Gamma_{N^*}(m)$, $\Gamma_{N^* \rightarrow \Delta\pi}(m)|_{l=0} = 0.2\Gamma_{N^*}(m)$, $\Gamma_{N^* \rightarrow \Delta\pi}(m)|_{l=2} = 0.15\Gamma_{N^*}(m)$, and $\Gamma_{N^* \rightarrow N\eta}(m)|_{l=2} = 2.3 \times 10^{-3}\Gamma_{N^*}(m)$.

For the $N^* \equiv N(1535)$ resonance,

$$\Gamma_{N^*}(m) = \Gamma_{N^* \rightarrow N\pi}(m)|_{l=0} + \Gamma_{N^* \rightarrow N\eta}(m)|_{l=0} + \Gamma_{N^* \rightarrow N\pi\pi}(m), \quad (12)$$

with $\Gamma_{N^* \rightarrow N\pi\pi}(m) = 0.1\Gamma_{N^*}(m)$ [25], $\Gamma_{N^* \rightarrow N\pi}(m)|_{l=0} = 0.48\Gamma_{N^*}(m)$, and $\Gamma_{N^* \rightarrow N\eta}(m)|_{l=0} = 0.42\Gamma_{N^*}(m)$.

For the $N^* \equiv N(1650)$ resonance,

$$\Gamma_{N^*}(m) = \Gamma_{N^* \rightarrow N\pi}(m)|_{l=0} + \Gamma_{N^* \rightarrow \Delta\pi}(m)|_{l=2} + \Gamma_{N^* \rightarrow N\eta}(m)|_{l=0}, \quad (13)$$

with $\Gamma_{N^* \rightarrow N\pi}(m)|_{l=0} = 0.75\Gamma_{N^*}(m)$, $\Gamma_{N^* \rightarrow \Delta\pi}(m)|_{l=2} = 0.15\Gamma_{N^*}(m)$, and $\Gamma_{N^* \rightarrow N\eta}(m)|_{l=0} = 0.1\Gamma_{N^*}(m)$.

For the $N^* \equiv N(1710)$ resonance,

$$\Gamma_{N^*}(m) = \Gamma_{N^* \rightarrow N\pi}(m)|_{l=1} + \Gamma_{N^* \rightarrow \Delta\pi}(m)|_{l=1} + \Gamma_{N^* \rightarrow N\eta}(m)|_{l=1} + \Gamma_{N^* \rightarrow \Lambda K}(m)|_{l=1}, \quad (14)$$

TABLE III. Blatt-Weisskopf barrier-penetration factor $B_l(\tilde{k}R)$ [26].

l	$B_l^2(x = \tilde{k}R)$
0	1
1	$x^2/(1+x^2)$
2	$x^4/(9+3x^2+x^4)$

with $\Gamma_{N^* \rightarrow N\pi}(m)|_{l=1} = 0.2\Gamma_{N^*}(m)$, $\Gamma_{N^* \rightarrow \Delta\pi}(m)|_{l=1} = 0.4\Gamma_{N^*}(m)$, $\Gamma_{N^* \rightarrow N\eta}(m)|_{l=1} = 0.3\Gamma_{N^*}(m)$, and $\Gamma_{N^* \rightarrow \Lambda K}(m)|_{l=1} = 0.1\Gamma_{N^*}(m)$.

For the $N^* \equiv N(1720)$ resonance,

$$\Gamma_{N^*}(m) = \Gamma_{N^* \rightarrow N\pi}(m)|_{l=1} + \Gamma_{N^* \rightarrow \Delta\pi}(m)|_{l=1} + \Gamma_{N^* \rightarrow N\eta}(m)|_{l=1} + \Gamma_{N^* \rightarrow \Lambda K}(m)|_{l=1}, \quad (15)$$

with $\Gamma_{N^* \rightarrow N\pi}(m)|_{l=1} = 0.11\Gamma_{N^*}(m)$, $\Gamma_{N^* \rightarrow \Delta\pi}(m)|_{l=1} = 0.75\Gamma_{N^*}(m)$, $\Gamma_{N^* \rightarrow N\eta}(m)|_{l=1} = 0.04\Gamma_{N^*}(m)$, and $\Gamma_{N^* \rightarrow \Lambda K}(m)|_{l=1} = 0.1\Gamma_{N^*}(m)$.

The partial decay width of a resonance, N^* , decaying to a baryon, B , and a meson, M , i.e., $\Gamma_{N^* \rightarrow BM}(m)|_l$, varies with its mass, m [26], as

$$\Gamma_{N^* \rightarrow BM}(m)|_l = \Gamma_{N^* \rightarrow BM}(m_{N^*}) \left[\frac{\Phi_l(m)}{\Phi_l(m_{N^*})} \right]. \quad (16)$$

The phase-space factor $\Phi_l(m)$ is given by $\Phi_l(m) = \frac{\tilde{k}}{m} B_l^2(\tilde{k}R)$, where \tilde{k} is the relative momentum of the decay products (i.e., B and M) in their center-of-mass frame. $B_l(\tilde{k}R)$ is the Blatt-Weisskopf barrier-penetration factor, listed in Table III. $R (= 0.25 \text{ fm})$ is the interaction radius.

The fivefold differential cross section of the considered reaction can be written as

$$\frac{d\sigma}{dE_{p'} d\Omega_{p'} d\Omega_{\eta}} = K_F \langle |T_{fi}|^2 \rangle, \quad (17)$$

where the annular brackets around $|T_{fi}|^2$ represent the average over spins in the initial state and the summation over spins in the final state. K_F is the kinematical factor for the reaction:

$$K_F = \frac{\pi}{(2\pi)^6} \frac{m_p^2 m_A k_p k_{\eta}^2}{k_p |k_{\eta}(E_i - E_{p'}) - E_{\eta} \mathbf{q} \cdot \hat{k}_{\eta}|}. \quad (18)$$

All symbols carry their usual meanings.

III. RESULTS AND DISCUSSION

The differential cross sections $\frac{d\sigma}{dE_{p'} d\Omega_{p'} d\Omega_{\eta}}$ have been calculated for the coherent η -meson energy E_{η} distribution in the (p, p') reaction on ^{14}C , a scalar-isovector nucleus. To describe the plane-wave results, χ s in T matrices in Eqs. (7) and (9) are given by $\chi^{(+)}(\mathbf{k}_p, \mathbf{r}) = e^{i\mathbf{k}_p \cdot \mathbf{r}}$ for the beam proton p , and $\chi^{(-)*}(\mathbf{k}_X, \mathbf{r}) = e^{-i\mathbf{k}_X \cdot \mathbf{r}}$ for a particle in the final state, i.e., X is either the ejectile proton p' or the η meson. The resonance nucleus interaction or optical potential $V_{ON^*}(\mathbf{r})$ is not considered at this stage. The spatial density distribution $\varrho(\mathbf{r})$ of the ^{14}C nucleus, as extracted from the electron scattering data [27], is given by

$$\varrho(\mathbf{r}) = \varrho_0 [1 + w(r/c)^2] e^{-(r/c)^2}, \quad w = 1.38, \quad c = 1.73 \text{ fm}. \quad (19)$$

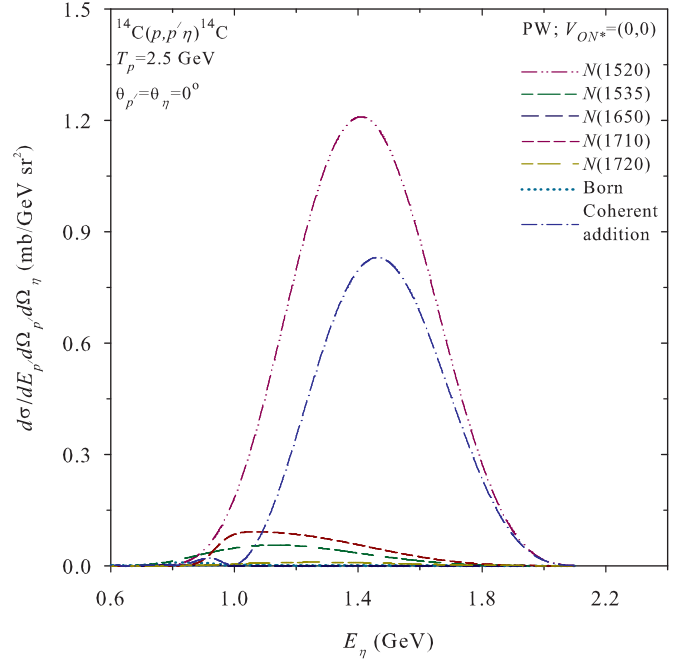


FIG. 2. (Color online) The η -meson energy E_{η} distribution spectra for the ^{14}C nucleus at 2.5 GeV. The cross section due to the $N(1520)$ resonance is distinctly the largest (dot-dot-dashed curve). The coherently added cross section (dot-dashed curve) is less than the previous cross section because of the interference of the Born terms and resonances quoted in the figure.

This density distribution is normalized to the mass number of the nucleus.

The isospin-averaged nuclear density distribution $\varrho_I(\mathbf{r})$, appearing in Eqs. (7) and (9), is related to $\varrho(\mathbf{r})$ as

$$\varrho_I(\mathbf{r}) = \left[\frac{Z}{A} C_{is}(p) + \frac{(A-Z)}{A} C_{is}(n) \right] \varrho(\mathbf{r}), \quad (20)$$

where $C_{is}(p)$ and $C_{is}(n)$ are the isospin matrix elements for the proton and the neutron, respectively. $C_{is}(p) = +1$ and $C_{is}(n) = -1$ are the values for the π^0 -meson exchange potential; both of them are equal to $+1$ for the η -meson exchange potential.

The calculated plane-wave (V_{ON^*} not included) results at 2.5 GeV are illustrated in Fig. 2. The coherent contribution of π^0 - and η -meson exchange potentials, i.e., $V_{\pi^0}(q)$ and $V_{\eta}(q)$, are incorporated in these results. This figure represents the cross sections due to Born terms and resonances (mentioned earlier) and the cross section occurring due to their coherent contributions. The dot-dot-dashed curve in this figure shows that the cross section because of the $N(1520)$ resonance is distinctly the largest. Compared to it, the cross sections due to Born terms and other resonances are insignificant. The interferences of Born terms and resonances in the coherently added cross section, presented by the dot-dashed curve, is visible in the figure. The peak of this cross section arises close to that due to the $N(1520)$ resonance.

The cross sections of the considered reaction due to $V_{\pi^0}(q)$ and $V_{\eta}(q)$ at 2.5 GeV are described in Fig. 3. Along with them, the coherently added cross section due to these potentials is

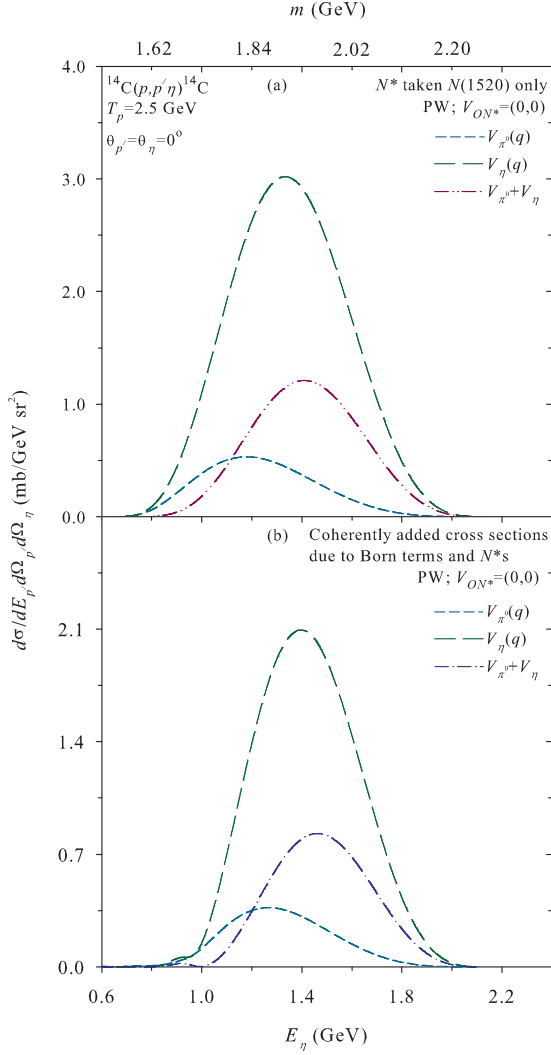


FIG. 3. (Color online) (a) Contributions of π^0 - and η -meson exchange potentials to the cross section arising due to the $N(1520)$ resonance only. The peak position is shifted to the higher value of E_η because of the interference of these potentials (dot-dot-dashed curve). (b) Same as those presented in the panel (a) but for the coherently added cross sections due to Born terms and resonances (see text).

also presented in this figure. Figure 3(a) shows the calculated results (plane wave; V_{ON^*} not included) arising due to the $N(1520)$ resonance only, because the cross section due to this resonance (as shown in the previous figure) is distinctly the largest. The cross section due to V_{π^0} (short-dashed curve) is significantly smaller ($\sim \frac{1}{5}$) than that due to V_η (large-dashed curve). The interference of these potentials is noticeable in the coherently added cross section (see dot-dot-dashed curve in this figure).

The smaller cross section arising due to the π^0 -meson exchange potential V_{π^0} over that due to the η -meson exchange potential V_η may be understood, as an initial thought, by analyzing the ratios of various factors appearing in $|\frac{V_{\pi^0}(q)}{V_\eta(q)}|^2$ at the respective peaks of the cross sections. The coupling constants, quoted below Eqs. (1) and (3), show the ratio $|\frac{g_{\pi^0} f_\pi^*}{g_\eta f_\eta^*}|^2$

is approximately equal to 1.23. The ratio of isospin matrix elements in $|\frac{V_{\pi^0}(q)}{V_\eta(q)}|^2$ is $\frac{1}{49}$, as the isospin contribution of a proton cancels that of a neutron in the nucleus for $V_{\pi^0}(q)$. Referring to Fig. 3(a), the peak cross section due to $V_{\pi^0}(q)$ appears at the four-momentum transfer $q^2 \simeq -0.18 \text{ GeV}^2$, whereas that due to $V_\eta(q)$ arises at $q^2 \approx -0.25 \text{ GeV}^2$. The form factors at the respective peaks, according to Eq. (5), are $F_\pi(q^2 \simeq -0.18 \text{ GeV}^2) = F_\pi^*(q^2 \simeq -0.18 \text{ GeV}^2) \simeq 0.89$ and $F_\eta(q^2 \approx -0.25 \text{ GeV}^2) = F_\eta^*(q^2 \approx -0.25 \text{ GeV}^2) \simeq 0.78$.

These values give $|\frac{F_\pi(q^2)}{F_\eta(q^2)}|^4 \simeq 1.7$. The values of the pseudoscalar meson propagators are $G_\pi(q^2 \simeq -0.18 \text{ GeV}^2) \simeq -5.06 \text{ GeV}^{-2}$ and $G_\eta(q^2 \approx -0.25 \text{ GeV}^2) \approx -1.83 \text{ GeV}^{-2}$, which show $|\frac{G_\pi(q^2)}{G_\eta(q^2)}|^2 \approx 7.65$. The product of these factors shows $|\frac{V_{\pi^0}(q)}{V_\eta(q)}|^2 \simeq \frac{1}{3.06}$, but the calculated results show the peak cross section due to V_η is ~ 5 larger than that due to V_{π^0} .

To resolve the above discrepancy (i.e., a factor of ~ 1.63), the $N^*(m) \rightarrow N\eta$ decay probabilities [for $N^* \equiv N(1520)$] at the peaks quoted in the previous analysis are considered. It is noticeable in Fig. 3(a) that the peak cross section due to V_{π^0} appears at $E_\eta \simeq 1.18 \text{ GeV}$, which corresponds to the resonance mass $m \approx 1.83 \text{ GeV}$, as mentioned on the upper x axis of this figure. The peak of the cross section due to V_η appears at $m \simeq 1.9 \text{ GeV}$. The ratio of the decay probabilities at the respective peaks, $\frac{\Gamma_{N^* \rightarrow N\eta}(m \approx 1.83 \text{ GeV})|_{V_{\pi^0}}}{\Gamma_{N^* \rightarrow N\eta}(m \approx 1.9 \text{ GeV})|_{V_\eta}}$, according to Eq. (16), is close to $\frac{1}{1.61}$. Therefore, the above analyses justify the lesser cross section due to V_{π^0} over that due to V_η , as is visible in Fig. 3(a).

The importance of V_{π^0} and V_η in the coherently added cross sections due to Born terms and quoted resonances is presented in Fig. 3(b). These spectra show features which are qualitatively similar to those elucidated in Fig. 3(a). This occurs because the distinctly dominant cross section, as mentioned earlier, arises because of the $N(1520)$ resonance.

To include the hadron nucleus interaction (optical potential) in the calculated cross section, the distorted wave functions are used for χ s in T matrices [given in Eqs. (7) and (9)] and G_{N^*} in Eq. (10) is replaced by the in-medium resonance propagator. Using the Glauber model [28,29], χ for the beam proton p can be written as

$$\chi^{(+)}(\mathbf{k}_p, \mathbf{r}) = e^{i\mathbf{k}_p \cdot \mathbf{r}} \exp \left[-\frac{i}{v_p} \int_{-\infty}^z dz' V_{Op}(\mathbf{b}, z') \right]. \quad (21)$$

For outgoing particles, i.e., p' and η meson, the form for the distorted wave functions is

$$\chi^{(-)*}(\mathbf{k}_X, \mathbf{r}) = e^{-i\mathbf{k}_X \cdot \mathbf{r}} \exp \left[-\frac{i}{v_X} \int_z^{+\infty} dz' V_{OX}(\mathbf{b}, z') \right] \times (X = p', \eta). \quad (22)$$

In the above equations, v and $V(\mathbf{b}, z')$ represent the velocity and optical potential, respectively, of the continuum particle. These potentials describe the initial and final state interactions of the reaction.

Incorporating the resonance nucleus interaction $V_{ON^*}(\mathbf{r})$ in $G_{N^*}(m)$ given in Eq. (10), the resonance propagator in the

nucleus can be expressed as

$$G_{N^*}(m, \mathbf{r}) = \frac{1}{m^2 - m_{N^*}^2 + im_{N^*}\Gamma_{N^*}(m) - 2E_{N^*}V_{ON^*}(\mathbf{r})}, \quad (23)$$

where E_{N^*} is the energy of the resonance N^* .

The optical potential $V_{OX}(\mathbf{r})$, appearing in Eqs. (21)–(23), is calculated using the “ $t\rho(\mathbf{r})$ ” approximation [29], i.e.,

$$V_{OX}(\mathbf{r}) = -\frac{v_X}{2}[i + \alpha_{XN}]\sigma_i^{XN}\varrho(\mathbf{r}), \quad (24)$$

where the symbol X represents either a proton or a resonance N^* . v_X is the velocity of the particle X . α_{XN} denotes the ratio of the real part to the imaginary part of X -nucleon scattering amplitude f_{XN} , and σ_i^{XN} is the corresponding total cross section. To evaluate the proton nucleus optical potential, i.e., $V_{Op}(\mathbf{r})$ as well as $V_{Op'}(\mathbf{r})$, the energy-dependent experimentally determined values for α_{pN} and σ_i^{pN} have been used [30]. The measured values for N^* -nucleon scattering parameters, i.e., α_{N^*N} and $\sigma_i^{N^*N}$, are not available. To estimate them, $\alpha_{N^*N} \approx \alpha_{pN}$ and $\sigma_{el}^{N^*N} \approx \sigma_{el}^{pN}$ are taken since the elastic scattering dynamics of N^* can be assumed to be not much different from that of a proton [31]. For the reactive part of $\sigma_i^{N^*N}$, the dynamics of N^* can be considered to be the same as that of a nucleon at its kinetic energy enhanced by Δm , i.e., $\sigma_r^{N^*N}(T_{N^*N}) \approx \sigma_r^{N^*N}(T_{N^*N} + \Delta m)$. Here, Δm is the mass difference between the resonance and the nucleon. T_{N^*N} is the total kinetic energy in the N^*N center-of-mass system [31].

The η -meson optical potential $V_{O\eta}(\mathbf{r})$ is evaluated from its self-energy $\Pi_\eta(\mathbf{r})$ in the nucleus. The resonance hole contribution to $\Pi_\eta(\mathbf{r})$, according to Lopez Alvarado and Oset [16], can be written as

$$\begin{aligned} \Pi_\eta(\mathbf{r}) &= 2E_\eta V_{O\eta}(\mathbf{r}) = \sum_{N^*} |C(N^*)|^2 \\ &\times \frac{\varrho(\mathbf{r})}{m - m_{N^*} + \frac{i}{2}\Gamma_{N^*}(m) - V_{ON^*}(\mathbf{r}) + V_{ON}(\mathbf{r})}. \end{aligned} \quad (25)$$

The prefactor $|C(N^*)|^2$ in this equation depends on the N^* resonance used to evaluate $\Pi_\eta(\mathbf{r})$. The nucleon potential energy in the nucleus is taken as $V_{ON}(\mathbf{r}) = -50\varrho(\mathbf{r})/\varrho(0)$ MeV [16]. $\Pi_\eta(\mathbf{r})$ arising due to the nucleon-hole pair is worked out following that due to the π^0 meson (see page 157 in Ref. [22]).

The sensitivity of the calculated cross section to the hadron nucleus interaction is exhibited in Fig. 4. The large peak (shown in this figure) in the coherently added cross sections (arising because of Born terms and considered resonances as well as because of π^0 - and η -meson exchange potentials) is considered for this purpose. The dot-dashed curve represents the plane-wave (V_{ON^*} not included) cross section of the considered reaction (also shown earlier). The cross section is reduced by a factor of 3.74 because of the incorporation of the initial state interaction (ISI) (see the long-dashed curve). The short-dashed curve elucidates the calculated spectrum obtained after the inclusion of both the ISI and the FSI (final state interaction); i.e., it describes the distorted wave results where V_{ON^*} is not taken into consideration. The cross section

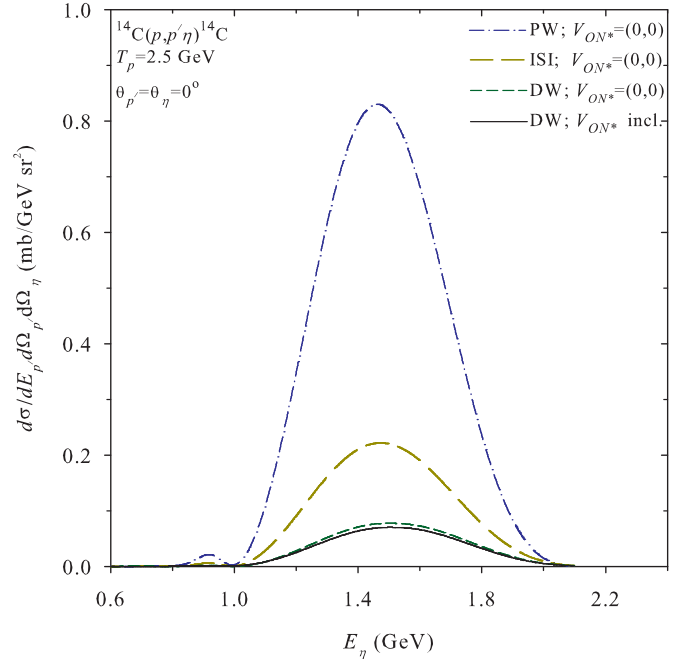


FIG. 4. (Color online) The sensitivity of the cross section to the hadron nucleus interaction (optical potential). The cross section is reduced drastically (by a factor of $\simeq 12$), and the peak position is shifted by 40 MeV towards the higher value of E_η because of these interactions.

is further reduced by a factor of 2.86 due to the inclusion of the FSI. The solid curve represents the calculated distorted wave results where V_{ON^*} has been incorporated. It shows the change in the cross section due to this potential is negligible.

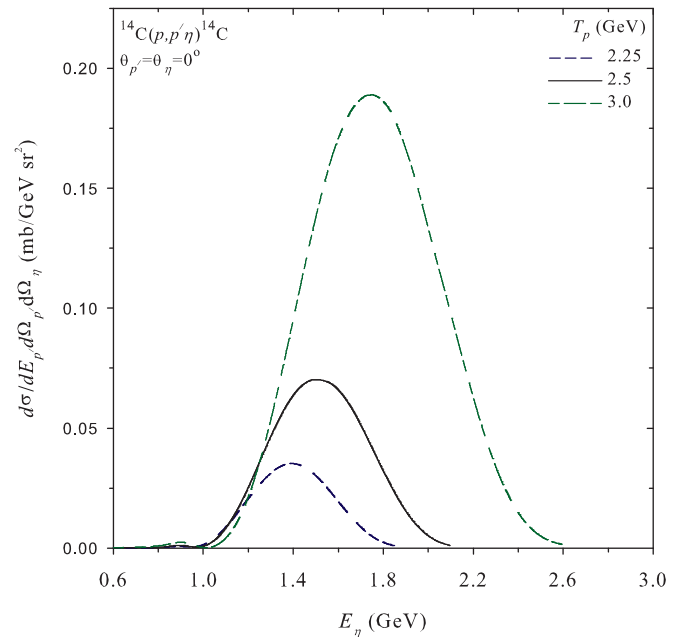


FIG. 5. (Color online) Beam energy dependence of the cross section. The cross section increases and the peak position shifts towards the higher E_η with the enhancement in the beam energy.

Therefore, the calculated plane-wave (V_{ON^*} not included) cross section is reduced drastically, i.e., by a factor of 11.81, because of the inclusion of all hadron nucleus interactions. The shift in the peak position because of these interactions is about 40 MeV towards the higher value of E_η in the spectrum.

The beam energy dependence of the distorted wave results is elucidated in Fig. 5. The resonance nucleus interactions are also included in these results. The cross section at the large peak is increased by a factor of 5.37, and the peak position is shifted from $E_\eta \simeq 1.39$ GeV to $E_\eta \simeq 1.75$ GeV with an increase in the beam energy from 2.25 to 3 GeV.

IV. CONCLUSIONS

Differential cross sections have been calculated for the coherent η -meson energy E_η distribution in the proton-induced reaction on a scalar-isovector nucleus. The η meson in the final state is considered to arise because of Born terms and resonances produced in the intermediate state. The interaction between the projectile proton and a nucleon in the target nucleus is described by the pseudoscalar meson (i.e., π^0 and η

meson) exchange potentials. The calculated results show that the distinctly dominant contribution to the η -meson production cross section arises because of the $N(1520)$ resonance. The coherently added cross section arising due to Born terms and considered resonances is less than the previous cross section due to their interferences. The cross section because of the π^0 -meson exchange potential is less than that due to the η -meson exchange potential. The interference of these potentials is distinctly visible in the η -meson energy E_η distribution spectrum. The cross section is reduced drastically and shifted towards higher E_η because of the hadron nucleus interactions, i.e., ISI and FSI including resonance nucleus interactions. The calculated results show that the cross section is very sensitive to the beam energy, because the magnitude of the cross section increases and its peak position shifts towards higher E_η with the enhancement in the beam energy.

ACKNOWLEDGMENTS

The author thanks the anonymous referee for giving comments those improved the quality of this work. Dr. L. M. Pant is acknowledged for his help in improving the manuscript.

-
- [1] V. Baru *et al.*, [arXiv:nucl-th/0610011](https://arxiv.org/abs/nucl-th/0610011).
- [2] S. Schadmand (for WASA at COSY Collaboration), *Pramana* **75**, 225 (2010).
- [3] J. Berger *et al.*, *Phys. Rev. Lett.* **61**, 919 (1988); R. Frascaria *et al.*, *Phys. Rev. C* **50**, R537 (1994).
- [4] J. C. Peng *et al.*, *Phys. Rev. Lett.* **63**, 2353 (1989).
- [5] W. B. Tippens *et al.*, *Phys. Rev. D* **63**, 052001 (2001).
- [6] F.-D. Berg *et al.*, *Phys. Rev. Lett.* **72**, 977 (1994).
- [7] M. Williams *et al.*, *Phys. Rev. C* **80**, 045213 (2009); B. Krusche *et al.*, *Phys. Rev. Lett.* **74**, 3736 (1995); J. W. Price *et al.*, *Phys. Rev. C* **51**, R2283(R) (1995); B. Krusche *et al.*, *Phys. Lett. B* **358**, 40 (1995); M. Röbig-Landau *et al.*, *ibid.* **373**, 45 (1996).
- [8] R. S. Bhalerao and L.-C. Liu, *Phys. Rev. Lett.* **54**, 865 (1985); Q. Haider and L.-C. Liu, *Phys. Lett. B* **172**, 257 (1986); L.-C. Liu and Q. Haider, *Phys. Rev. C* **34**, 1845 (1986); G. L. Li, W. K. Cheng, and T. T. S. Kuo, *Phys. Lett. B* **195**, 515 (1987).
- [9] R. E. Chrien *et al.*, *Phys. Rev. Lett.* **60**, 2595 (1988); A. Budzanowski *et al.* (COSY-GEM Collaboration), *Phys. Rev. C* **79**, 012201(R) (2009).
- [10] C. Y. Cheung, *Phys. Lett. B* **119**, 47 (1982); C. Wilkin, *ibid.* **331**, 276 (1994).
- [11] J. Lehr, M. Post, and U. Mosel, *Phys. Rev. C* **68**, 044601 (2003); J. Lehr and U. Mosel, *ibid.* **68**, 044603 (2003); R. C. Carrasco, *ibid.* **48**, 2333 (1993).
- [12] M. Hedayati-Poor and H. S. Sherif, *Phys. Rev. C* **76**, 055207 (2007); M. Hedayati-Poor, S. Bayegan, and H. S. Sherif, *ibid.* **68**, 045205 (2003).
- [13] Ch. Sauerma, B. L. Friman, and W. Nörenberg, *Phys. Lett. B* **341**, 261 (1995); J.-F. Germond and C. Wilkin, *Nucl. Phys. A* **518**, 308 (1990); A. Moalem, E. Gedalin, L. Razdolskaja, and Z. Shorer, *ibid.* **589**, 649 (1995).
- [14] J. M. Laget, F. Wellers, and J. F. Lecomte, *Phys. Lett. B* **257**, 254 (1991).
- [15] T. Vetter, A. Engel, T. Brió, and U. Mosel, *Phys. Lett. B* **263**, 153 (1991).
- [16] B. Lopez Alvaredo and E. Oset, *Phys. Lett. B* **324**, 125 (1994).
- [17] S. Das, *Phys. Lett. B* **737**, 75 (2014).
- [18] J. Beringer *et al.* (Particle Data Group), *Phys. Rev. D* **86**, 010001 (2012).
- [19] L.-C. Liu, J. T. Londergan, and G. E. Walker, *Phys. Rev. C* **40**, 832 (1989).
- [20] W. Peters, H. Lenske, and U. Mosel, *Nucl. Phys. A* **642**, 506 (1998).
- [21] I. R. Blokland and H. S. Sherif, *Nucl. Phys. A* **694**, 337 (2001).
- [22] T. Ericson and W. Weise, *Pions and Nuclei* (Clarendon, Oxford, 1988), p. 18.
- [23] H. C. Chiang, E. Oset, and L.-C. Liu, *Phys. Rev. C* **44**, 738 (1991); R. Machleidt, K. Holinde, and Ch. Elster, *Phys. Rep.* **149**, 1 (1987).
- [24] S. Das, *Phys. Rev. C* **70**, 034604 (2004).
- [25] G. Fäldt and C. Wilkin, *Nucl. Phys. A* **587**, 769 (1995); A. Fix and H. Arenhövel, *ibid.* **620**, 457 (1997).
- [26] D. M. Manley, R. A. Arndt, Y. Goradia, and V. L. Teplitz, *Phys. Rev. D* **30**, 904 (1984); D. M. Manley, *ibid.* **51**, 4837 (1995); *Int. J. Mod. Phys. A* **18**, 441 (2003).
- [27] C. W. De Jager, H. De Vries, and C. De Vries, *At. Data Nucl. Data Tables* **14**, 479 (1974).
- [28] R. J. Glauber, in *Lectures in Theoretical Physics*, edited by W. E. Brittin *et al.* (Interscience, New York, 1959), Vol. 1.
- [29] S. Das, *Phys. Rev. C* **72**, 064619 (2005).
- [30] D. V. Bugg *et al.*, *Phys. Rev.* **146**, 980 (1966); S. Barshay *et al.*, *Phys. Rev. C* **11**, 360 (1975); W. Grein, *Nucl. Phys. B* **131**, 255 (1977); C. Lechanoine-Leluc and F. Lehar, *Rev. Mod. Phys.* **65**, 47 (1993); R. M. Barnett *et al.* (Particle Data Group), *Phys. Rev. D* **54**, 1 (1996); <http://pdg.lbl.gov/xsect/contents.html>.
- [31] B. K. Jain, N. G. Kelkar, and J. T. Londergan, *Phys. Rev. C* **47**, 1701 (1993).